

## Suppression of Clock Shifts at Magnetic-Field-Insensitive Transitions

K. J. Arnold and M. D. Barrett\*

*Center for Quantum Technologies, 3 Science Drive 2, Singapore 117543, Singapore  
and Department of Physics, National University of Singapore,*

*2 Science Drive 3, Singapore 117551, Singapore*

(Received 7 June 2016; published 11 October 2016)

We show that it is possible to significantly reduce rank 2 tensor shifts of a clock transition by operating at a judiciously chosen magnetic-field-insensitive point. In some cases shifts are almost completely eliminated making the transition an effective  $J = 0$  to  $J = 0$  candidate. This significantly improves the feasibility of a recent proposal for clock operation with large ion crystals. For such multi-ion clocks, geometric constraints and selection rules naturally divide clock operation into two categories based on the orientation of the magnetic field. We discuss the limitations imposed on each type and how calibrations might be carried out for clock operation.

DOI: 10.1103/PhysRevLett.117.160802

The realization of accurate, stable frequency references has enabled important advances in science and technology. Increasing levels of accuracy and stability continue to be made with atomic clocks based on optical transitions in isolated atoms [1–9]. However, in the case of single ion clocks, further improvements in accuracy are hindered by their relatively low stability, which makes averaging times prohibitively long.

Recently, we have shown that ion clock candidates with a negative differential scalar polarizability  $\Delta\alpha_0$  could operate with large numbers of ions by utilizing a magic radio-frequency (rf) trap drive at which micromotion shifts cancel [10]. Of the candidates reported in the literature that have  $\Delta\alpha_0 < 0$ ,  $B^+$  [11],  $Ca^+$  [11],  $Sr^+$  [11],  $Ba^+$  [12],  $Ra^+$  [12],  $Er^{2+}$  [13],  $Tm^{3+}$  [13], and  $Lu^+$  [13], all but one involve clock states with  $J > 1/2$ , which introduces further perturbations of the clock transition from rank 2 tensor interactions. Methods used to cancel these shifts involve averaging over multiple transitions [14–16], or multiple field orientations [17]. In the case of many ions, this leads to inhomogeneous broadening, which imposes practical limitations to the probe interrogation time and the number of ions one can use [10]. It is therefore of interest to explore alternative methods to deal with shifts arising from this class of interactions.

Here, we focus on those  $\Delta\alpha_0 < 0$  candidates with an upper  $D$  state, specifically  $Ca^+$ ,  $Sr^+$ ,  $Ba^+$ ,  $Lu^+$ , and  $Lu^{2+}$ . We show that shifts from rank 2 tensor interactions can be practically eliminated by operating at a judiciously chosen field-insensitive point, at which the linear dependence of the transition frequency on the magnetic field vanishes. In the presence of a magnetic field, states are mixed through the Zeeman interaction, which alters the influence of rank 2 tensor interactions relative to the unmixed values. By example, we illustrate that each candidate has at least one clock transition that becomes field insensitive at a point at which rank 2 perturbations are substantially diminished.

The case of doubly ionized lutetium has not yet been considered as a viable clock candidate so we also include relevant clock considerations for this ion. We note that one is at liberty to define a clock frequency as the frequency of the experimentally convenient field-insensitive transition. In this case there is no need to extrapolate to a zero field but merely a need to quantify the root-mean-square deviations from the field-insensitive point.

For fixed  $J$ , the Zeeman interaction is given by

$$H_z = \frac{\mu_B B}{\hbar} (g_J J_z + g_I I_z) \quad (1)$$

with matrix elements

$$\begin{aligned} \langle (IJ)F', m_F | H_z | (IJ)F, m_F \rangle &= (g_J - g_I) \mu_B B (-1)^{J+I+1+m_F} J \sqrt{(2F'+1)(2F+1)} \\ &\times \begin{Bmatrix} F & F' & 1 \\ J & J & I \end{Bmatrix} \begin{pmatrix} J & 1 & J \\ -J & 0 & J \end{pmatrix}^{-1} \begin{pmatrix} F & 1 & F' \\ -m_F & 0 & m_F \end{pmatrix} \\ &+ g_I m_F \mu_B B \delta_{F,F'}, \end{aligned} \quad (2)$$

where we have included  $IJ$  in the state notation to specify the order of coupling  $I$  and  $J$ . The Zeeman interaction preserves  $m_F$  and eigenstates can be found by diagonalizing the Hamiltonian restricted to a manifold of fixed  $m_F$ . Provided perturbations from rank 2 tensor interactions remain small relative to the spacing between energy levels, shifts can be calculated as an expectation value using the new eigenstates. At low field, a rank 2 perturbation factors into three terms: a state-dependent scalar coefficient depending on the angular momentum quantum numbers typically on the order of unity, which we refer to as the shift coefficient and denote by  $C_2$ , a scalar parameter depending on the properties of the atom that determines the coupling strength of the interaction for the particular fine structure level, and a geometry dependent term that depends only on

the strength of the applied fields and their orientation relative to the quantization axis. Since the Zeeman interaction preserves  $m_F$ , this separation remains intact provided there is no accidental near degeneracy with neighboring Zeeman manifolds. However,  $C_2$  must properly take into account the mixing induced by the Zeeman interaction. For a given state, the coefficient is determined by the expectation value of the  $m_F$ -dependent matrix with matrix elements given by

$$H_{F',F} = (-1)^{J+I+m_F} \sqrt{(2F'+1)(2F+1)} \\ \times \begin{Bmatrix} F & F' & 2 \\ J & J & I \end{Bmatrix} \begin{pmatrix} J & 2 & J \\ -J & 0 & J \end{pmatrix}^{-1} \\ \times \begin{pmatrix} F & 2 & F' \\ -m_F & 0 & m_F \end{pmatrix}. \quad (3)$$

Matrix elements of the tensor polarizability are given by

$$\langle F', m_F | H_E | F, m_F \rangle = -\frac{1}{4} H_{F',F} \alpha_{2,J} \langle 3E_z^2 - |E|^2 \rangle, \quad (4)$$

where  $\alpha_{2J}$  is the frequency dependent tensor polarizability for the fine-structure level of interest, and  $\langle \cdot \rangle$  denotes a time average. Similarly, matrix elements for the quadrupole operator are given by

$$\langle F', m_F | H_Q | F, m_F \rangle \\ = H_{F',F} \Theta(J) A [(3\cos^2\beta - 1) - \epsilon \sin^2\beta (\cos^2\alpha - \sin^2\alpha)], \quad (5)$$

where  $\Theta(J)$  is the quadrupole moment of the fine structure level of interest,  $A$  and  $\epsilon$  characterize the strength of the applied field gradients, and  $\alpha$  and  $\beta$  are the Euler angles determining the orientation of the electric field gradient with respect to the quantization axis [17]. We note that general matrix elements for the polarizability are given in Ref. [18] and a slight generalization of the treatment given in Ref. [17] can be used to show they have the same form for the quadrupole interaction. The matrix elements given in Ref. [19] differ from those given in Ref. [18] due to a different ordering of  $I$  and  $J$ .

For a given atom, it is a simple matter to exhaustively search for field-insensitive points of the clock transition and determine  $C_2$  by the expectation value of the matrix given in Eq. (3). In Fig. 1, we illustrate the near coincidence of a field-insensitive point and a zero shift coefficient for  $^{43}\text{Ca}^+$ . Further examples for each candidate are given in Table I where we give the zero-field states associated with the transition, the shift coefficient, and the quadratic Zeeman shift at the field-insensitive point. The table is by no means exhaustive, at least for some of the candidates, and we have listed the most promising transitions for each.

Where possible, analysis is based on experimentally determined hyperfine splittings and this is the case for  $^{43}\text{Ca}^+$ ,  $^{137}\text{Ba}^+$ , and  $^{175}\text{Lu}^+$ . For  $^{87}\text{Sr}^+$ , the experimental

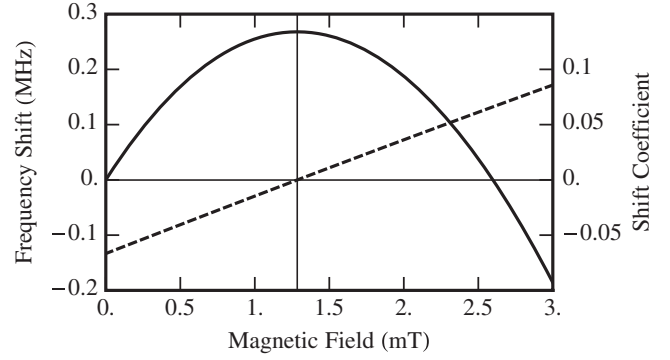


FIG. 1. The magnetic field dependence of the  $|S_{1/2}, 4, -3\rangle$  to  $|D_{3/2}, 5, -3\rangle$  transition in  $^{43}\text{Ca}^+$ . The solid curve shows the frequency dependence of the transition relative to the zero-field value with the vertical line marking the field-insensitive point of approximately 1.28 mT. The dashed curve shows the field dependence of the corresponding shift coefficient with the horizontal line marking the intercept at the field-insensitive point giving a shift coefficient  $C_2 \approx -5.8 \times 10^{-5}$ .

value in Ref. [21] for the  $S_{1/2}$  level is used but calculations given in Ref. [22] are used for the  $D_{3/2}$  level. Similarly, we have relied upon calculations of the hyperfine structure for  $^{175}\text{Lu}^{2+}$  [25]. For  $^{176}\text{Lu}^+$ , we have used experimental values for  $^{175}\text{Lu}^+$  to determine the hyperfine  $A$  and  $B$  coefficients and rescaled them based on measured nuclear magnetic dipole and electric quadrupole moments. The results given in Table I have varying levels of sensitivity to calculated values. However, in general, the Hamiltonian describing Zeeman mixing of the upper state can be scaled by the largest separation of the hyperfine states. This simply sets a scale for the magnetic field and does not change the form of the eigenenergies and eigenstates as a function of the scaled field. In as much as the hyperfine splittings are described by the hyperfine  $A$  and  $B$  coefficients, the rescaled Hamiltonian then depends only on the ratio  $B/A$  and this dependence is typically rather weak. Moreover, for relevant field values, the ground-state energies are well described by a comparatively weak quadratic form. Hence, the existence of such coincident points is reasonably robust to small changes in the calculated hyperfine structure.

The case of singly ionized lutetium is unique in that it is the only candidate that has no hyperfine structure in the ground state. The simple structure of the  $^3D_1$  level does not yield any coincident points and, in fact, the field-insensitive points typically coincide with extrema in the values of  $C_2$ . This is also the case for  $^{175}\text{Lu}^+$  on the  $^3D_2$  line but it just so happens the extremal value of  $C_2$  is also small. However, this is not the case for  $^{176}\text{Lu}^+$  on the  $^3D_2$  line. In this case there is a much stronger variation of  $C_2$  with the magnetic field and it has a higher sensitivity to changes in the hyperfine structure compared to other transitions listed in the table.

TABLE I. Field-insensitive transitions at which the shift coefficient,  $C_2$ , that scales the rank 2 tensor perturbations, is small. Transitions are identified by their zero-field quantum numbers. All transitions are  $S_{1/2}$  to  $D_{3/2}$  with the exception of  $\text{Lu}^+$  which is an  $^1S_0$  to  $^3D_2$  transition. The value of the magnetic field,  $B_0$ , at which the transition becomes field insensitive is given in column 3, and the quadratic dependence is given in column 4. In the final column references from which the hyperfine structure was determined are given.

Element	Transition	$B_0$ (mT)	$\alpha_Z$ (kHz/mT <sup>2</sup> )	$C_2$	References
$^{43}\text{Ca}^+$	$ 4, 0\rangle \leftrightarrow  3, -2\rangle$	0.051	58.8	-0.006	[20]
$^{43}\text{Ca}^+$	$ 4, -3\rangle \leftrightarrow  5, -3\rangle$	1.28	-159	$-5.8 \times 10^{-5}$	[20]
$^{87}\text{Sr}^+$	$ 4, -3\rangle \leftrightarrow  3, -1\rangle$	5.34	304	-0.004	[21,22]
$^{87}\text{Sr}^+$	$ 4, 0\rangle \leftrightarrow  4, 0\rangle$	12.8	69.0	0.030	[21,22]
$^{137}\text{Ba}^+$	$ 2, 1\rangle \leftrightarrow  2, 0\rangle$	53.1	-70.0	-0.066	[23,24]
$^{175}\text{Lu}^{2+}$	$ 4, 3\rangle \leftrightarrow  5, 3\rangle$	20.8	9.7	$-5.6 \times 10^{-4}$	[25]
$^{175}\text{Lu}^{2+}$	$ 4, -3\rangle \leftrightarrow  2, -2\rangle$	73.6	30.8	0.005	[25]
$^{175}\text{Lu}^+$	$ 7/2, -1/2\rangle \leftrightarrow  9/2, -1/2\rangle$	56.6	22.1	-0.035	[26]
$^{176}\text{Lu}^+$	$ 7, -5\rangle \leftrightarrow  6, -5\rangle$	521	29.8	-0.007	[26]

The case of  $^{43}\text{Ca}^+$  offers a unique possibility at a low field due to the nuclear spin of  $I = 7/2$ . In this case the  $6J$  symbol in Eq. (2) vanishes for  $F = F' = 3$ . Thus, the  $g$  factor for the  $F = 3$  upper state is given by the nuclear  $g$  factor  $g_I$ . It is also the case that the expectation value of any rank 2 tensor vanishes for an angular momentum state  $|3, \pm 2\rangle$ . Hence, at low fields, these states are inherently free of any significant Zeeman, quadrupole, or tensor polarizability shifts. Furthermore, the quadratic Zeeman shifts of the  $|3, \pm 2\rangle$  states are anomalously small owing to the small hyperfine  $B$  coefficient for  $^{43}\text{Ca}^+$ . Indeed, the quadratic shift for the transition  $|4, 0\rangle$  to  $|3, -2\rangle$  is almost entirely due to the ground state. With the very small linear Zeeman shift, the transition becomes field insensitive at approximately 50  $\mu\text{T}$ . This field gives a small amount of Zeeman mixing, which accounts for the shift coefficient of  $-0.006$  given in the table.

The result for the  $|4, -3\rangle \leftrightarrow |5, -3\rangle$  transition in  $^{43}\text{Ca}^+$  is also a consequence of the  $I = 7/2$  nuclear spin. In this case the difference in  $g$  factors for the two states is just 0.01. This provides a field-insensitive point at low field, which can be treated within the framework of perturbation theory. Neglecting the quadratic dependence of the ground state, the magnetic field value at the field-insensitive point is linear in the hyperfine separation of the  $F = 4$  and 5 upper levels. To the same approximation, the mixing of the two upper levels at the field-insensitive point is independent of the hyperfine separation and the zero-field shift coefficient of  $C_2 = -1/15$  is shifted to  $\approx -0.0083$ . Including the quadratic dependence of the ground state decreases the quadratic dependence of the transition and increases the magnetic field at the field-insensitive point. The associated increase in Zeeman mixing brings  $C_2$  to approximately zero. The same calculation applies to the corresponding transition in  $^{175}\text{Lu}^{2+}$  with a sign change in  $m$  corresponding to a sign change of the nuclear magnetic moment. Similar reasoning also applies to the  $|4, -3\rangle \leftrightarrow |3, -1\rangle$  transition in  $^{87}\text{Sr}^+$  although this transition involves

a stronger mixing of the upper states. Consequently, for all three of these transitions, the  $C_2$  coefficient is insensitive to exact values of the hyperfine splittings.

In the sequence of alkaline-earth ions, the differential scalar polarizability  $\Delta\alpha_0$  becomes increasingly negative with increasing atomic mass. Doubly ionized lutetium takes the role of a heavy alkaline-earth-like ion but the extra ion charge offsets this trend. From published matrix elements [27], we estimate  $\Delta\alpha_0 \approx -20.7$  with a tensor contribution of  $\alpha_{2,J} = -5.2$  where both results are given in atomic units. As the scalar polarizabilities of the ground and excited states are significantly different (28.0 and 7.3, respectively), we expect the estimate of  $\Delta\alpha_0$  to be reasonable. Using the flexible atomic code [28], we have calculated the lifetime of the  $D_{3/2}$  level to be approximately 160 s. The long lifetime, together with the near vanishing shift coefficient of the  $|4, -3\rangle \leftrightarrow |5, -3\rangle$  transition, makes this a particularly interesting candidate for a multi-ion clock.

In the multi-ion clock proposal [10], clock interrogation along the rf null axis of a linear Paul trap is required to avoid micromotion-induced depletion of the probe coupling. For the  $E2$  transitions considered here, selection rules constrain the orientation of the magnetic field that one can use. This leads to two types of operation: one in which the field is aligned to the trap axis, and the other in which it is rotated by a nonzero angle. The former only applies to those transitions with  $|\Delta m| = 1$  but in either case, the ultimate performance will depend on the alignment of the magnetic field with respect to the trap axis.

With the Euler angles  $\alpha$  and  $\beta$  as defined in Eq. (5), the tensor polarizability shift due to an rf electric field with amplitude  $\mathbf{E} = (E_x, E_y, 0)$  is given by

$$\frac{\delta\nu}{\nu} = -\frac{C_2\alpha_{2,J}}{4h\nu} \left( -\frac{1}{4}(3\cos^2\beta - 1)|\mathbf{E}|^2 + \frac{3}{4}\sin^2\beta[\cos 2\alpha(E_x^2 - E_y^2) - 2\sin 2\alpha E_x E_y] \right), \quad (6)$$

where we have assumed the rf field to be purely transverse to the trap axis as considered in Ref. [10]. In a Coulomb crystal, the second term in Eq. (6) has a mean value of zero, provided  $\langle E_x^2 \rangle = \langle E_y^2 \rangle$ , and gives a number-dependent inhomogeneous broadening of the line. In a spherically symmetric crystal, the broadening would be symmetric and would not give rise to additional shifts associated with changes to the line shape. Small differences in  $\langle E_x^2 \rangle$  and  $\langle E_y^2 \rangle$  could be tolerated by setting  $\alpha = \pi/4$ , which means the projection of the magnetic field on the  $xy$  plane is at  $45^\circ$  to both the  $x$  and  $y$  axis. The first term in Eq. (6) has a mean value proportional to  $N^{2/3}$ . This gives rise to a number-dependent shift of the transition.

When the field is aligned to the trap axis, the number-dependent broadening can be compensated by a slight adjustment of the magic rf frequency [10]. The only other broadening mechanism is from the crystal-induced quadrupole shifts, which are independent of number and heavily reduced by  $C_2$ . From the analysis given in Ref. [10] and the values of  $C_2$  given in Table I, this broadening would be  $\sim 1$  mHz and likely not observable. In practice, one would simply increase the number of ions, tuning the rf frequency to eliminate variations in the clock frequency with number, and tuning the field alignment to null any observable number-dependent broadening. Hence, this operation allows for arbitrary levels of stability with only a residual quadrupole shift induced by dc electric field gradients. Since the magnetic field would be calibrated to the trap axis, the dominant contribution from the dc confinement could be calibrated by measuring the trap frequencies. We note that for  $C_2 \sim 1$  typical quadrupole shifts are  $\sim 1$  Hz [17]. For the candidates given in Table I, we would then anticipate fractional frequency shifts of  $\lesssim 10^{-17}$ , which should easily allow uncertainties below  $10^{-18}$ . Contributions from stray fields need not be aligned with the trap axis but we would expect these to be significantly smaller than the applied fields.

Off-axis operation is needed when  $|\Delta m| = 0, 2$ . Assuming the magic rf frequency has been precalibrated by another method, the orientation of the magnetic field can then be tuned so that  $3 \cos^2 \beta - 1 = 0$  by eliminating any observable number-dependent shifts in the clock frequency. From Eq. (5), the magnetic field would also be oriented such that the residual quadrupole shift arising from the dc confinement fields is also canceled. Errors in the value of the magic rf frequency will lead to errors in field alignment and a shift of the clock frequency from the dc confinement field. Further quadrupole shifts from stray dc fields will arise as before and we would expect similar levels of inaccuracies as the previous case.

For off-axis operation, number-dependent broadening limits the achievable stability. The broadening scales quadratically with the size of the crystal, which scales as  $N^{1/3}$ . The maximum interrogation time then scales as  $N^{-2/3}$  leading to an instability with a weak  $N^{-1/6}$  scaling. For all

practical purposes this can be considered constant once the broadening begins to degrade the Ramsey fringe or the line shape. For the spherically symmetric case considered in Ref. [10], the broadening is characterized by

$$\Delta\nu = \frac{C_2}{4} \left| \frac{\alpha_{2,J}}{\Delta\alpha_0} \right| \left( \frac{Z^2 \alpha \hbar \omega_z}{mc^2} \right)^{2/3} \nu N^{2/3}, \quad (7)$$

where  $\alpha$  is the fine structure constant,  $Z$  is the charge number of the ion,  $\omega_z$  is the trapping frequency along the axial direction, and  $\nu$  is the clock frequency. Based on simulations, the fringe contrast is reduced to  $\sim 80\%$  for a Ramsey time of  $1/(2\pi\Delta\nu)$ . Thus, Eq. (7) provides an effective bound on the number of ions for a given interrogation time. The dependence on  $\Delta\alpha_0$  arises because it determines the magic rf frequency, which, in turn, determines the strength of the electric field needed for a particular confinement. In terms of broadening, this favors candidates in which the ratio  $\alpha_{2,J}/\Delta\alpha_0$  is small. For  $^{43}\text{Ca}^+$  and  $^{175}\text{Lu}^{2+}$  these considerations are largely irrelevant with the very small  $C_2$  value providing an effective  $J = 0$  to  $J = 0$  transition. Indeed, for  $^{175}\text{Lu}^{2+}$ , a Ramsey time of 1 s would limit the number to  $N \gtrsim 10^6$  with an instability  $\sigma(1\text{s}) < 10^{-18}$ , where we have taken  $\omega_z = 2\pi \times 200$  kHz. Clearly, other factors will limit the stability well before such extremes are reached.

In conclusion, we have shown that field-insensitive points of clock transitions may be found at which perturbations from rank 2 tensor interactions are significantly diminished. In the case of  $^{175}\text{Lu}^{2+}$ , this approach provides a clock candidate that is essentially field free except for a 9.7 kHz/mT<sup>2</sup> quadratic Zeeman shift. Although this is large relative to other clock candidates it must be remembered that clock operation would be at the field-insensitive point so that only rms field variations need to be accounted for. This approach significantly improves the feasibility of a recent proposal for clock operation with large ion crystals. We also note that our approach need not be restricted to ions and may well be useful for neutral atoms in optical lattices.

We would like to thank W.R. Johnson and U.I. Safronova for providing us with initial calculations of the hyperfine structure constants for  $^{175}\text{Lu}^{2+}$ . This research is supported by the National Research Foundation, Prime Minister's Office, Singapore and the Ministry of Education, Singapore under the Research Centres of Excellence program. It is also supported in part by an A\*STAR SERC 2015 Public Sector Research Funding (PSF) Grant (SERC Project No: 1521200080).

*Note added*—Recently, calculations for this atom have been published [29]. The numbers agree well with the values used here and give a reduction in the magnitude of the  $C_2$  coefficient given in the table.

- \*phybmd@nus.edu.sg
- [1] C. W. Chou, D. B. Hume, J. C. J. Koelemeij, D. J. Wineland, and T. Rosenband, *Phys. Rev. Lett.* **104**, 070802 (2010).
- [2] B. J. Bloom, T. L. Nicholson, J. R. Williams, S. L. Campbell, M. Bishof, X. Zhang, W. Zhang, S. L. Bromley, and J. Ye, *Nature (London)* **506**, 71 (2014).
- [3] J. E. Stalnaker, S. Diddams, T. Fortier, K. Kim, L. Hollberg, J. Bergquist, W. Itano, M. Delany, L. Lorini, W. Oskay, T. Heavner, S. Jefferts, F. Levi, T. Parker, and J. Shirley, *Appl. Phys. B* **89**, 167 (2007).
- [4] P. Dube, A. A. Madej, Z. Zhou, and J. E. Bernard, *Phys. Rev. A* **87**, 023806 (2013).
- [5] N. Huntemann, M. Okhapkin, B. Lipphardt, S. Weyers, C. Tamm, and E. Peik, *Phys. Rev. Lett.* **108**, 090801 (2012).
- [6] Y. H. Wang, R. Dumke, T. Liu, A. Stejskal, Y. Zhao, J. Zhang, Z. Lu, L. J. Wang, T. Becker, and H. Walther, *Opt. Commun.* **273**, 526 (2007).
- [7] Z. W. Barber, C. W. Hoyt, C. W. Oates, L. Hollberg, A. V. Taichenachev, and V. I. Yudin, *Phys. Rev. Lett.* **96**, 083002 (2006).
- [8] A. D. Ludlow, M. M. Boyd, J. Ye, E. Peik, and P. Schmidt, *Rev. Mod. Phys.* **87**, 637 (2015).
- [9] N. Hinkley, J. A. Sherman, N. B. Phillips, M. Schioppo, N. D. Lemke, K. Beloy, M. Pizzocaro, C. W. Oates, and A. D. Ludlow, *Science* **341**, 1215 (2013).
- [10] K. Arnold, E. Hajiyev, E. Paez, C. H. Lee, M. D. Barrett, and J. Bollinger, *Phys. Rev. A* **92**, 032108 (2015).
- [11] M. S. Safronova, M. G. Kozlov, and C. W. Clark, *IEEE Trans. Ultrason. Ferroelectr. Freq. Control* **59**, 439 (2012).
- [12] B. K. Sahoo, R. G. E. Timmermans, B. P. Das, and D. Mukherjee, *Phys. Rev. A* **80**, 062506 (2009).
- [13] A. Kozlov, V. A. Dzuba, and V. V. Flambaum, *Phys. Rev. A* **90**, 042505 (2014).
- [14] M. D. Barrett, *New J. Phys.* **17**, 053024 (2015).
- [15] P. Dubè, A. A. Madej, J. E. Bernard, L. Marmet, J.-S. Boulanger, and S. Cundy, *Phys. Rev. Lett.* **95**, 033001 (2005).
- [16] S. Schiller, D. Bakalov, and V. I. Korobov, *Phys. Rev. Lett.* **113**, 023004 (2014).
- [17] W. M. Itano, *J. Res. Natl. Inst. Stand. Technol.* **105**, 829 (2000).
- [18] B. Arora, M. S. Safronova, and C. W. Clark, *Phys. Rev. A* **76**, 052509 (2007).
- [19] F. L. Kien, P. Schneeweiss, and A. Rauschenbeutel, *Eur. Phys. J. D* **67**, 92 (2013).
- [20] J. Benhelm, G. Kirchmair, U. Rapol, T. Körber, C. F. Roos, and R. Blatt, *Phys. Rev. A* **75**, 032506 (2007).
- [21] H. Sunaoshi, Y. Fukashiro, M. Furukawa, M. Yamauchi, S. Hayashibe, T. Shinozuka, M. Fujioka, I. Satoh, M. Wada, and S. Matsuki, *Hyperfine Interact.* **78**, 241 (1993).
- [22] U. I. Safronova, *Phys. Rev. A* **82**, 022504 (2010).
- [23] R. Blatt and G. Werth, *Phys. Rev. A* **25**, 1476 (1982).
- [24] N. C. Lewty, B. L. Chuah, R. Cazan, and M. D. Barrett, *Opt. Express* **20**, 21379 (2012).
- [25] W. R. Johnson and U. I. Safronova (private communication). They have provided  $A(S_{1/2}) = 13158.4$  MHz,  $A(D_{3/2}) = 504.7$  MHz and  $B(D_{3/2}) = 1957.4$  MHz.
- [26] H. Schüler and H. Gollnow, *Z. Phys.* **113**, 1 (1939).
- [27] P. P. E. Biémont, Z. S. Li, and P. Quinet, *J. Phys. B* **32**, 3409 (1999).
- [28] M. Gu, *Can. J. Phys.* **86**, 675 (2008).
- [29] U. I. Safronova, M. S. Safronova, and W. R. Johnson, *Phys. Rev. A* **94**, 032506 (2016).